Optimal Energy Management of Unbalanced Three-Phase Grid-Connected Microgrids

Juan S. Giraldo, Jhon A. Castrillon
and Carlos A. Castro, *Senior Member, IEEE*
School of Electrical and Computer Engineering
University of Campinas
Campinas, São Paulo, Brazil

Federico Milano, *Fellow, IEEE*
School of Electrical and Electronic Engineering
University College Dublin
Dublin, Ireland

***Abstract*—This paper presents a non-linear optimization problem based on nodal current injections to solve the optimal energy management of unbalanced, three-phase, grid-connected microgrids. The focus is on the modelling of small synchronous machines under unbalanced operation. Inverter-interfaced distributed energy resources, i.e., renewable sources and energy storage systems, are also considered and described. The proposed formulation minimizes the cost of the energy consumed by the microgrid while satisfying active and reactive power balances, the devices operational constraints, as well as current and voltage operational limits. The proposed model is tested using the IEEE 123 node test feeder and compared to commonly used formulations. Simulation results show the impact of unbalanced models on the energy management of three-phase microgrids.**

***Index Terms*—Optimal energy management, unbalanced microgrid, unbalanced generator model, renewable energy sources.**

I. Introduction

A. Motivation

A grid-connected microgrid consists of a group of loads serviced by a distribution main grid, along with a cluster of distributed energy resources (DERs) and energy storage systems (ESSs), providing economic, reliable, and secure electric power to its consumers [1]. The optimal energy management (OEM) of microgrids consists in finding the optimal power injection from dispatchable distributed generator (DG) units and the management of ESSs to achieve selected objectives. These objectives include the minimization of operating costs, system losses, imported energy, environmental footprint, among others, and must be achieved while maintaining technical and operational constraints [2].

While there exist several studies on the optimal operation of microgrids, there are still aspects peculiar to their modelling that have not been considered so far. This work aims at evaluating the impact of synchronous machines models and power unbalances in the OEM of microgrids.

This study was financed in part by the Coordenação de Aperfeiçoamento de Pessoal de Nível Superior – Brasil (CAPES) – Finance Code 001, and the Brazilian National Council for Scientific and Technological Development (CNPq).

Federico Milano is supported by Science Foundation Ireland, under Grant No. SFI/15/SPP/E3125 and Grant No. SFI/15/IA/3074.

B. Literature Review

Several approaches have been proposed for solving the OEM problem of microgrids. In [3], a centralized energy management system is proposed based on the forecasted values of loads and non-dispatchable generation units. In [4], a heuristic approach is introduced to solve the power dispatch of microsources. In [5], a multiobjective single-step formulation dispatch of DG units and ESSs is proposed based on a niching evolutionary algorithm. A load management model is proposed in [6] to improve microgrid resilience following islanding. The authors in [7] propose a robust energy management for grid-connected and islanding microgrids considering an AC approach.

The aforementioned models are focused on single-phase equivalents, and most of them consider active power only. Unlike high-voltage networks, distribution systems and microgrids cannot be usually assumed to be balanced. Unbalances are associated with line configurations, i.e., untransposed, with two-phase and single-phase laterals, and to the characteristics of the loads, where single-phase and two-phase connections prevail. These features require the use of three-phase models for the network and its devices, thus, increasing the size and complexity of the problem [8].

The OEM of microgrids considering three-phase configurations has also been the subject of several studies. In [9] a non-linear programming model is proposed for the optimal scheduling of distributed resources in microgrids applying different objective functions. Reference [10] proposes a centralized dispatch for a set of non-synchronous microgrids pursuing loss reduction and unbalance compensation. Reference [11] proposes a mixed-integer linear programming model for unbalanced microgrids considering unexpected main grid outages. The power injection from DG units has been commonly modeled using balanced power sources, as in [12] and [13], as single-phase machines in [14], or considering each phase's power as controllable variables [11], just to mention some.

The models proposed in the literature above do not consider the physical coupling of power flows between phases for calculating the power injected into the system by synchronous machines. An energy management system for three-phase,

island-mode microgrids considering unbalanced synchronous machines is proposed in [15]. However, this approach does not consider the reactive power balance to obtain the optimal solution.

C. Contributions

This paper proposes a mathematical model for the OEM of unbalanced, grid-connected microgrids considering the steady-state model of small synchronous machines under unbalanced operation. The proposed formulation accounts for DG units, ESS and renewable energy sources (RES) in an AC approach, filling a gap in the current literature for this kind of models. The proposed formulation is tested through the unbalanced IEEE 123 nodes test feeder using AMPL [16] and solved with the non-linear solver Knitro [17] under default settings. The results obtained with the proposed model are compared with two alternative approaches, commonly used in the literature to assess the effectiveness of using approximated models in unbalanced systems.

II. Proposed Formulation

The proposed OEM consists in finding the optimal participation of each dispatchable source to the power balance, i.e., substation imports and dispatchable DGs units, as well as the appropriate state of charge (SOC) of every ESS while integrating non-dispatchable sources into the network. Moreover, the system must guarantee a secure operation at all times by keeping the state variables within limits, such as nodal voltage magnitudes, substation maximum capacity, DG units' operational limits, line thermal ratings, and secure SOC limits. The resulting model is formulated as a non-linear programming problem, as follows:

$$\begin{cases} \min\ f(\mathbf{V},\,\mathbf{I}) & (2) \\ \text{s.t.}\quad h(\mathbf{V},\,\mathbf{I})=0 & (3)\text{–}(12) \\ \qquad g(\mathbf{V},\,\mathbf{I})\le 0 & (13)\text{–}(19) \end{cases} \tag{1}$$

The proposed model minimizes the total energy cost over a period of time, discretized in a finite number of time-steps $t \in \Omega_{\mathrm{T}}$ each lasting $\Delta\mathrm{t}$ hours:

$$f(\mathbf{V},\,\mathbf{I}) = \sum_{t\in\Omega_{\mathrm{T}}} \Delta\mathrm{t} \left(c_t^{\mathrm{s}}\, \Re\left\{ \mathbf{V}_{s,t}{}^{\mathsf{T}} \mathbf{I}_{s,t}^{s\,*} \right\} + \sum_{g\in\Omega_{\mathrm{G}}} c_g^{\mathrm{dg}} P_{g,t}^{dg} \right) \tag{2}$$

where the first term considers the cost of the energy imported from the main grid weighted with c_t^{s}, while the second one stands for the injected energy from the dispatchable DGs in the set Ω_{G}, with c_g^{dg} standing for the unitary cost and $P_{g,t}^{dg}$ for the injected active power. The current injected by the substation must be set to zero for all buses but the substation bus (s), i.e, $\mathbf{I}_{i,t}^{s}{}^{\mathsf{T}} = [0,\,0,\,0]\ \forall\ i \in \Omega_{\mathrm{B}},\ t \in \Omega_{\mathrm{T}}\ |i \neq s$. Similarly, three-phase nodal voltages at the substation, which are used as reference, must be fixed as $\mathbf{V}_{s,t}{}^{\mathsf{T}} = \left[1,\,a^2,\,a\right]\ \forall\ t \in \Omega_{\mathrm{T}}$, where $a = e^{j2\pi/3}$ hereinafter.

The nodal current balance is expressed in complex form in (3), where $\mathbf{Y}_{i,j}$ is the (3×3) admittance submatrix of the branch joining nodes i and j, both belonging to the set of buses Ω_{B}. $\mathbf{I}_{i,t}^{N}$ and $\mathbf{V}_{j,t}$ are column vectors comprising the three-phase complex components of net currents and nodal voltages, respectively, as follows:

$$\mathbf{I}_{i,t}^{N} = \sum_{j\in\Omega_{\mathrm{B}}} \mathbf{Y}_{i,j}\mathbf{V}_{j,t} \qquad \forall\, i\in\Omega_{\mathrm{B}},\, t\in\Omega_{\mathrm{T}} \tag{3a}$$

$$\mathbf{I}_{i,t}^{N} = \sum_{g\in\Omega_{\mathrm{G}}|g=i} \mathbf{I}_{g,t}^{dg} + \sum_{e\in\Omega_{\mathrm{E}}|e=i} \mathbf{I}_{e,t}^{es} + \sum_{w\in\Omega_{\mathrm{R}}|w=i} \mathbf{I}_{w,t}^{rw} + \mathbf{I}_{i,t}^{s} - \mathbf{I}_{i,t}^{ld} \tag{3b}$$

The net current at node i, $\mathbf{I}_{i,t}^{N}$, comprises the current injection from dispatchable DGs grouped in set Ω_{G}, ESS in set Ω_{E}, RES in Ω_{R}, and finally the current injection from the substation and from loads. The island-mode operation of microgrids can be included by adding a load shedding penalty to the objective function and the respective modification to the current balances as in [18].

A. Loads and renewable energy sources

Electric power demand is an input parameter based on a previous forecast stage as in [19], in which, the expected power consumption $\mathbf{S}_{i,t}^{\mathrm{ld}}$ is obtained. A similar assumption can be made for renewable sources, which in this paper are assumed as photovoltaic (PV) units, where the expected power can be forecasted as in [20], and represented by $\mathbf{S}_{w,t}^{\mathrm{rw}}$. Nodal currents from loads and RES can be calculated as:

$$\mathbf{I}_{i,t}^{ld\,*} = \mathbf{diag}\left(\mathbf{V}_{i,t}\right)^{-1}\ \mathbf{S}_{i,t}^{\mathrm{ld}} \qquad \forall\, i\in\Omega_{\mathrm{B}},\, t\in\Omega_{\mathrm{T}} \tag{4}$$

$$\mathbf{I}_{w,t}^{rw\,*} = \mathbf{diag}\left(\mathbf{V}_{w,t}\right)^{-1}\ \mathbf{S}_{w,t}^{\mathrm{rw}} \qquad \forall\, w\in\Omega_{\mathrm{R}},\, t\in\Omega_{\mathrm{T}} \tag{5}$$

where $\mathbf{diag}\left(\cdot\right)$ represents a diagonal matrix containing the elements of the vector.

B. Dispatchable distributed generators (Model 1)

Dispatchable DG units are often synchronous cogenerators or microturbines that, in distribution systems, are not subject to voltage control and maintain constant power injections. This is why they are often represented as PQ injections [21]. The model used to represent a DG unit in steady state is shown in Fig. 1, where the Thevenin equivalent of the synchronous machine is modeled as a balanced voltage source in series with an admittance matrix $\mathbf{Y}_{\mathbf{G}_g}$. V_g^{bal} is a complex number representing the machine's armature voltage magnitude and the load angle. The admittances of the generators are represented by means of conventional sequence components:

$$\mathbf{A} = \begin{bmatrix} 1 & 1 & 1 \\ 1 & a^2 & a \\ 1 & a & a^2 \end{bmatrix} \qquad \mathbf{Y}_{\mathbf{G}_g} = \mathbf{A} \begin{bmatrix} z_g^0+3z_g^n & 0 & 0 \\ 0 & z_g^1 & 0 \\ 0 & 0 & z_g^2 \end{bmatrix}^{-1} \mathbf{A}^{-1} \tag{6}$$

where z_g^n stands for the grounding impedance. The positive sequence impedance is approximated with the direct-axis synchronous reactance $z_g^1 \approx jx_g^d$. Saliency and internal resistances are neglected. Similarly, the negative sequence impedance is expressed as a function of the unsaturated subtransient reactances as $z_g^2 \approx j\left(x_g^{d''} + x_g^{q''}\right)/2$. The zero sequence is expressed as $z_g^0 \approx z_g^2/4$ [22], [23]. The current and the power injected by a DG located at bus $g\in\Omega_{\mathrm{G}}$ is expressed as:

$$\mathbf{I}_{g,t}^{dg} = \mathbf{Y}_{\mathbf{G}_g}\left(V_{g,t}^{bal}\begin{bmatrix}1\\ a^2\\ a\end{bmatrix} - \mathbf{V}_{g,t}\right), \qquad \forall\, g\in\Omega_{\mathrm{G}},\, t\in\Omega_{\mathrm{T}} \tag{7}$$

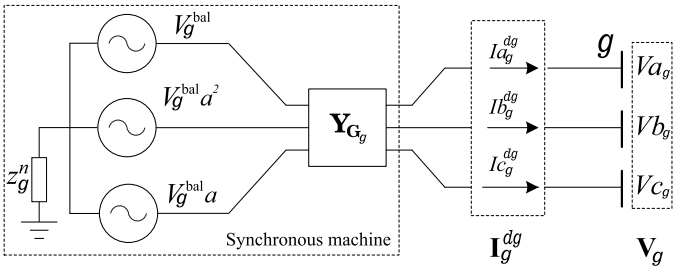

Fig. 1. Unbalanced dispatchable distributed generator model.

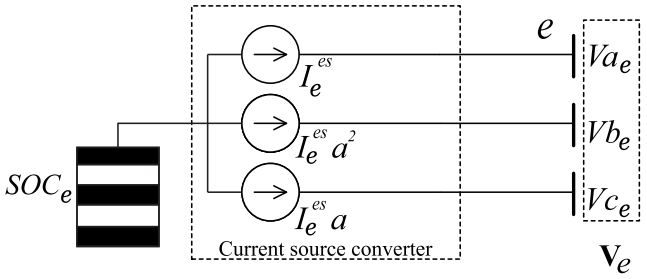

Fig. 2. Energy storage system model.

$$P_{g,t}^{dg} = \Re\left\{\mathbf{V}_{g,t}{}^{\mathsf{T}}\, \mathbf{I}_{g,t}^{dg\,*}\right\}, \qquad \forall\, g \in \Omega_{\mathrm{G}},\, t \in \Omega_{\mathrm{T}} \quad (8)$$

$$Q_{g,t}^{dg} = \Im\left\{\mathbf{V}_{g,t}{}^{\mathsf{T}}\, \mathbf{I}_{g,t}^{dg\,*}\right\}, \qquad \forall\, g \in \Omega_{\mathrm{G}},\, t \in \Omega_{\mathrm{T}} \quad (9)$$

where the three-phase currents injected to the system by the DG are determined by (7), while (8) and (9) define the injected active and reactive three-phase power components, respectively. Note that the proposed model for dispatchable DGs in unbalanced networks is independent on the status of the microgrid; thus, it is also suitable for island-mode operation.

C. Energy storage systems

ESSs are connected to the microgrid through power electronic converters. These are controlled to inject or to absorb power in a four-quadrant operation, allowing for reactive power compensation if needed. Although power electronic converters are usually modeled as voltage-sources, several modelling control approaches, such as [24] and [25], suggest the use of current-source converters (CSCs) in order to inject balanced currents to the system. The schematic of the ESS model as a CSC is shown in Fig. 2.

Three-phase active and reactive powers are expressed as a function of the current injected or consumed by an ESS at node $e \in \Omega_{\mathrm{E}}$ as:

$$P_{e,t}^{es} = \Re\left\{\mathbf{V}_{e,t}{}^{\mathsf{T}}\, I_{e,t}^{es\,*} \begin{bmatrix} 1 \\ a \\ a^2 \end{bmatrix}\right\}, \qquad \forall\, e \in \Omega_{\mathrm{E}},\, t \in \Omega_{\mathrm{T}} \quad (10)$$

$$Q_{e,t}^{es} = \Im\left\{\mathbf{V}_{e,t}{}^{\mathsf{T}}\, I_{e,t}^{es\,*} \begin{bmatrix} 1 \\ a \\ a^2 \end{bmatrix}\right\}, \qquad \forall\, e \in \Omega_{\mathrm{E}},\, t \in \Omega_{\mathrm{T}} \quad (11)$$

where $I_{e,t}^{es}$ is a complex number. Furthermore, the current SOC of each ESS is calculated as:

$$SOC_{e,t} = (1 - \xi_e)\, SOC_{i,t-1} - \frac{\Delta \mathrm{t}}{\mathrm{EC}_e}\left(P_{e,t}^{es}\, \eta_e\right) \qquad \forall\, e \in \Omega_{\mathrm{E}},\, t \in \Omega_{\mathrm{T}} \quad (12)$$

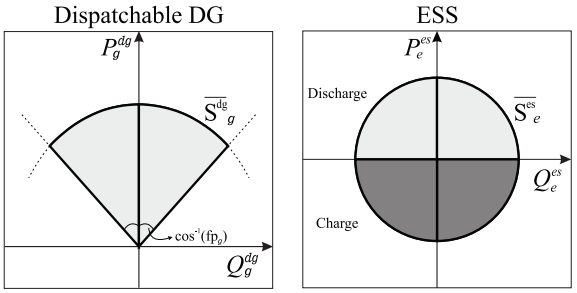

Fig. 3. Operational limits for dispatchable DG units and ESS.

considering an initial charge $SOC_{e,0}$, the self discharge rate of the storage system ξ_e, its efficiency η_e, and its total energy capacity EC_e. As can be inferred from (12), the status of the ESS is defined as discharging if $P_{e,t}^{es} > 0$ or as charging if $P_{e,t}^{es} < 0$.

D. Operational Limits

Operational limits for dispatchable power generation devices, i.e., DG and ESS, have to be taken into account in order to obtain a feasible solution. Similarly, system's operational limits such as maximum current magnitude through distribution lines, maximum and minimum nodal voltage magnitudes, and the rated power for the transformer connecting the microgrid to the main grid, must also be considered and can be modeled as:

$$\left(P_{g,t}^{dg}\right)^2 + \left(Q_{g,t}^{dg}\right)^2 \le \left(\overline{\mathrm{S}^{\mathrm{dg}}}_g\right)^2, \qquad \forall g \in \Omega_{\mathrm{G}}, t \in \Omega_{\mathrm{T}} \quad (13)$$

$$P_{g,t}^{dg} \tan\left(\cos^{-1}\left(\mathrm{pf}_g\right)\right) \ge |Q_{g,t}^{dg}|, \qquad \forall\, g \in \Omega_{\mathrm{G}},\, t \in \Omega_{\mathrm{T}} \quad (14)$$

$$\underline{\mathrm{SOC}}_e \le SOC_{e,t} \le \overline{\mathrm{SOC}}_e, \qquad \forall\, e \in \Omega_{\mathrm{E}},\, t \in \Omega_{\mathrm{T}} \quad (15)$$

$$\left(P_{e,t}^{es}\right)^2 + \left(Q_{e,t}^{es}\right)^2 \le \left(\overline{\mathrm{S}^{\mathrm{es}}}_e\right)^2, \qquad \forall\, e \in \Omega_{\mathrm{E}},\, t \in \Omega_{\mathrm{T}} \quad (16)$$

$$|\mathbf{Y}_{i,j}\left(\mathbf{V}_{i,t} - \mathbf{V}_{j,t}\right)| \le \bar{\mathrm{I}}_{i,j}, \quad \forall\, i,\, j \in \Omega_{\mathrm{B}},\, t \in \Omega_{\mathrm{T}} |\, i \ne j \quad (17)$$

$$\underline{\mathrm{V}} \le |\mathbf{V}_{i,t}| \le \overline{\mathrm{V}}, \qquad \forall\, i \in \Omega_{\mathrm{B}},\, t \in \Omega_{\mathrm{T}} \quad (18)$$

$$\left|\mathbf{V}_{i,t}{}^{\mathsf{T}} \mathbf{I}_{i,t}^{s\,*}\right| \le \overline{\mathrm{S}^{\mathrm{s}}}, \qquad \forall i \in \Omega_{\mathrm{B}}, t \in \Omega_{\mathrm{T}} | i = s \quad (19)$$

where $|\cdot|$ stands for the element-wise complex modulus. The capability of each dispatchable DG unit is guaranteed by (13), which limits the maximum apparent power injected, $\overline{\mathrm{S}^{\mathrm{dg}}}_g$, and by (14), which limits the maximum reactive power the machine can withstand depending on the parameter pf_g. The maximum and minimum values allowed for the SOC of each ESS are respectively $\overline{\mathrm{SOC}}_e$ and $\underline{\mathrm{SOC}}_e$ as in (15). Equation (16) limits the maximum apparent power of each ESS, defined as $\overline{\mathrm{S}^{\mathrm{es}}}_e$. A graphical representation of the operational limits for dispatchable DG units and ESS is shown in Fig. 3. The thermal limit of the distribution lines is accounted for in (17), where $\bar{\mathrm{I}}_{i,j}$ is the maximum rated current of each line, as well as minimum and maximum limits for nodal voltage magnitudes in (18), represented by $\underline{\mathrm{V}}$ and $\overline{\mathrm{V}}$, respectively. Finally, the rated power of the substation is constrained by (19), where $\overline{\mathrm{S}^{\mathrm{s}}}$ represents the maximum apparent power flowing through the substation.

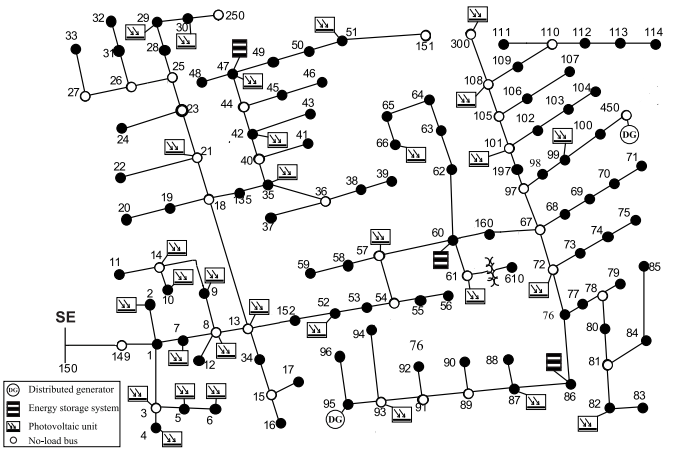

Fig. 4. Case study microgrid based on the modified IEEE 123 node test feeder.

III. Case study

The test system of Fig. 4 represents a modified version of the 123-bus 4.16 kV distribution test feeder discussed in [26]. An hourly analysis is proposed, with a time step $\Delta t = 1.0$ h, where the highest demand period takes place at $t = 20$ h, with 1,420 kW consumed in phase a, 915 kW in phase b, and 1,155 kW in phase c. Two dispatchable DGs are assumed to be installed in the system, along with three ESSs characterized as shown in Table I. PV units are assumed to be installed in 30 nodes with a peak power of 66 kWp each, at unitary power factor. The maximum allowable power for the substation was set to $\overline{\mathrm{S^s}} = 3.0$ MVA, voltage magnitude limits assumed as $\underline{\mathrm{V}} = 0.95$ p.u and $\overline{\mathrm{V}} = 1.05$ p.u. The thermal ratings of distribution lines are set considering the cable configurations of the original system. The sequence impedances for synchronous machines are arbitrarily set based on usual ranges, i.e., $z_g^1 = [80 - 150]$ % and $z_g^2 = [11 - 35]$ %, referred to the unit's base power. Also, ESSs are constrained to complete the day with their initial charge.

Three models representing dispatchable DG units based on synchronous machines are compared, namely, Model 1 for the proposed model considering unbalanced conditions, Model 2 for balanced power injections, and Model 3 for a balanced voltage source in series with a diagonal matrix representing the direct axis synchronous reactance of each phase z_g^1, assuming no coupling between phases.

The voltage magnitude at node 114, phase a, and the current magnitude at branch 150-149, also for phase a, are shown in Fig. 5 for all time periods. Results obtained with the three models are compared to a reference scenario where no dispatchable DG units or ESS are considered and no limits are enforced. The minimum voltage limit is violated at heavy load periods (around $t = 20$ h). A similar result is obtained for the current magnitude of the distribution line, where the maximum rated current is violated. When DG units and ESS are added, both magnitudes are held between the limits. The highest voltages and lower currents are obtained with Model 1,

TABLE I
Parameters of ESS and DG units

Device	Parameter	Value	Unit
DG units	$\overline{\mathrm{S^{dg}}}_g$	350	kVA
	pf_g	0.9	-
	z_g^1	110.0	%
	z_g^2	20.0	%
	c_g^{dg}	0.14	$/kW
ESS	$\overline{\mathrm{S^{es}}}_e$	200	kVA
	ξ_e	1	%
	$\overline{\mathrm{SOC}}_e$	100	%
	$SOC_{e,0}$	98	%
	$\underline{\mathrm{SOC}}_e$	10	%
	EC_e	1.0	MWh
	η_e	95	%

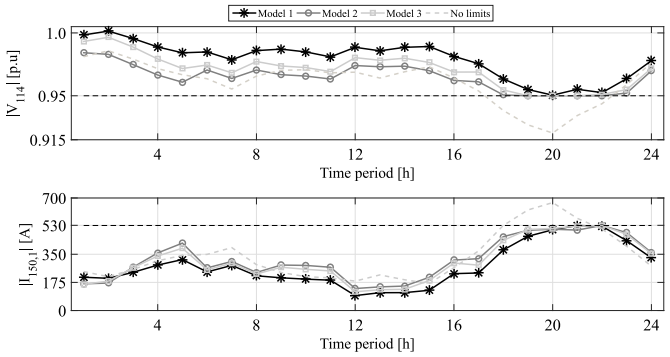

Fig. 5. Voltage magnitude at bus 114 and current magnitude at line 150-149 considering different synchronous machine models for DG units.

whereas Model 2 leads to the lowest voltage and highest current magnitudes. These results are directly related to the power injections of dispatchable DG units, shown in Fig. 6, where these units behave differently depending on the model used for representing the synchronous machines. Notice that the power injected using Model 1 (left bar) is higher than the one injected with the other two models for almost all periods, justifying the higher voltage profile at node 114 and lower current from the substation. However, during heavy load conditions, i.e., $t = \{19, 20\}$ h, the power injected using Model 2 (center bar) present the highest values, followed closely by Model 3 (right bar).

The main difference between the three models relies upon the ability of Model 1 of accounting for possible unbalances in the power injected from synchronous machines, which is a physical consequence of its connection into unbalanced networks. The active and reactive power injected by each phase of the DG unit at node 450 is shown in Fig. 7 for the three models. The injected active powers using Model 1 are not equal in all phases, being higher in phase a and lower in phase b. Moreover, although the overall three-phase reactive power is positive, as shown in Fig. 6, the reactive power injection in phase b is negative indicating an inductive behavior, whereas phases a and c inject reactive power to the system. Contrarily,

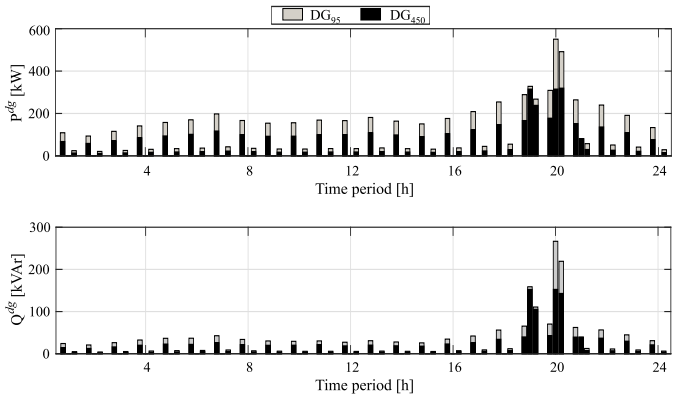

Fig. 6. Three-phase active and reactive power injected by the DG units with different machine models: Model 1 (left bar), Model 2 (center bar), and Model 3 (right bar).

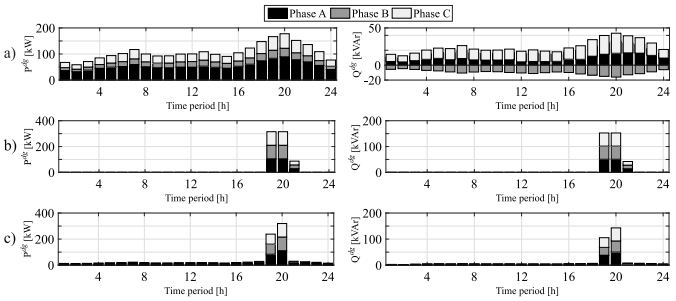

Fig. 7. Active and reactive powers per phase injected by the DG unit at bus 450 using: a) Model 1, b) Model 2, and c) Model 3.

Model 2 injects the same amount of power in each phase only in high demand periods with a leading power factor, while Model 3 also shows a leading factor but the powers injected at each phase are not equal. Figure 6 also shows that Model 2 and Model 3 have a similar general behavior in all periods, regardless the differences due to the use of a balanced power source in the former and a balanced voltage source in the latter.

Figure 8 shows the SOC of the storage system at node 47 and the three-phase active power injected/absorbed to/from the network. Although the three models behave in a similar way, Model 1 shows a more conservative operation up to period 16, followed by a deeper discharge compared to the other two models, and finishes, as demanded by the operator, with the initial charge at the end of the day. The differences in the charging and discharging patterns of the ESS are a direct consequence of the redistribution of the power flows in the system, which is caused only by considering different models for synchronous machines.

Figure 9 shows the energy injected by all sources, i.e., the substation, dispatchable DG units, PV units, and ESS for Model 1. The substation represents the biggest share of energy during most periods. However, PV units account for an important part during daylight hours, especially around midday. The total energy from ESS follow the same behavior shown in Fig. 8, with a deep discharge during periods 17-20,

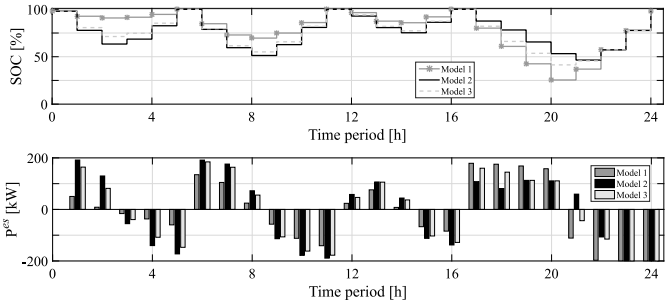

Fig. 8. SOC and three-phase active power injected by the ESS at node 47 considering different synchronous machine models for DG units.

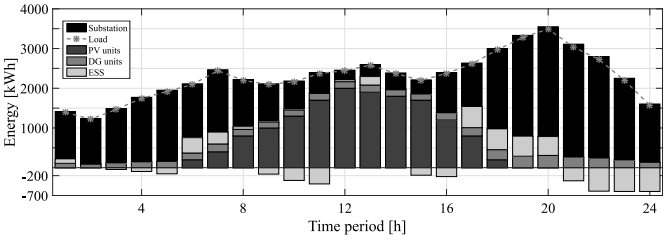

Fig. 9. Total energy injected by sources and consumed by loads - Model 1.

where negative values represent charging. Finally, the energy injected by DG units corresponds to a small share, but it is necessary for maintaining the operational variables within their limits.

Table II compares the results obtained using the tested models for dispatchable DG units considering the objective function cost, total energy losses, number of iterations to converge, and total computational time. The highest cost for the objective function is obtained using Model 1 which is approximately 17% more expensive than Model 2, and 14% higher than Model 3. As expected, the less expensive solution is obtained when no limits are enforced, indicating a less constrained operational point. However, the total energy lost behaves in the opposite way, as DG units using Model 1 share more energy during the day than the other tests, redistributing the power flows. The number of iterations and the total execution time show a marked difference between the reference case and the other three simulations, suggesting an increase in the computational burden due to the addition of the non-linear equations describing DG units and ESS. Furthermore, Model 1, which is the most detailed model of the three, performs about 9% faster than Model 2 and 19% faster than Model 3. This result, although unexpected, can be explained by the non-convexity of the problem and by specific characteristics of the tested system.

IV. Conclusions

This paper proposes a mathematical model for the optimal energy management of unbalanced, three-phase, grid-connected microgrids based on nodal current injections. A steady-state model for dispatchable DG units considering the unbalanced behavior of small synchronous machines con-

TABLE II
PERFORMANCE OF THE TESTED SIMULATIONS

	Cost [$]	Losses [kWh]	Iterations	Time [s]
No limits	1571.08	849.79	3	0.534
Model 1	1985.85	706.67	20	2.019
Model 2	1647.90	777.81	22	2.204
Model 3	1707.81	775.28	24	2.417

nected to three-phase systems is included in the formulation. The model for DG units is compared with two different approaches commonly used in the literature, one assuming balanced power injections and the other one ignoring the coupling between phases.

The effect of the tested models on the charging/discharging patterns of ESS has been discussed, as well as some differences in the objective function costs, total energy losses, and computational burden. Although all tested models lead to feasible solutions, results showed that ignoring the coupling between phases in synchronous machines for the OEM of unbalanced microgrids may lead to optimistic results, where the energy costs are lower. Results also show that ignoring the coupling between phases in synchronous machines does not result in an improvement on the computational burden, not justifying the use of approximated models.

Future work will consider different unbalance scenarios, island-mode operation, as well as the stochasticity of exogenous parameters, such as the power from renewable sources and conventional loads.

REFERENCES

[1] R. H. Lasseter and P. Paigi, "Microgrid: a conceptual solution," in *2004 IEEE 35th Annual Power Electronics Specialists Conference*, Aachen, Germany, 20–25 Jun., 2004, pp. 4285–4290.

[2] F. Katiraei, R. Iravani, N. Hatziargyriou, and A. Dimeas, "Microgrids management," *IEEE Power Energy Magazine*, vol. 6, no. 3, pp. 54–65, May 2008.

[3] D. E. Olivares, C. A. Cañizares, and M. Kazerani, "A centralized optimal energy management system for microgrids," in *2011 IEEE PES General Meeting*, San Diego, CA, 24–29 Jul, 2011.

[4] E. Alvarez, A. C. Lopez, J. Gómez-Aleixandre, and N. de Abajo, "Online minimization of running costs, greenhouse gas emissions and the impact of distributed generation using microgrids on the electrical system," in *IEEE PES/IAS Conference on Sustainable Alternative Energy*, Valencia, Spain, 28-30 Sep., 2009.

[5] S. Conti, R. Nicolosi, S. A. Rizzo, and H. H. Zeineldin, "Optimal dispatching of distributed generators and storage systems for mv islanded microgrids," *IEEE Transactions on Power Delivery*, vol. 27, no. 3, pp. 1243–1251, Jul. 2012.

[6] C. Gouveia, J. Moreira, C. L. Moreira, and J. A. P. Lopes, "Coordinating storage and demand response for microgrid emergency operation," *IEEE Transactions on Smart Grid*, vol. 4, no. 4, pp. 1898–1908, Dec. 2013.

[7] J. S. Giraldo, J. A. Castrillon, J. C. López, M. J. Rider, and C. A. Castro, "Microgrids energy management using robust convex programming," *IEEE Transactions on Smart Grid*, to be published.

[8] D. Shirmohammadi, H. Hong, A. Semlyen, and G. Luo, "A compensation-based power flow method for weakly meshed distribution and transmission networks," *IEEE Transactions on Power Systems*, vol. 3, no. 2, pp. 753–762, May 1988.

[9] G. Carpinelli, F. Mottola, D. Proto, and P. Varilone, "Minimizing unbalances in low-voltage microgrids: Optimal scheduling of distributed resources," *Applied Energy*, vol. 191, pp. 170–182, Apr. 2017.

[10] T. Hong and F. de León, "Centralized unbalanced dispatch of smart distribution dc microgrid systems," *IEEE Transactions on Smart Grid*, vol. 9, no. 4, pp. 2852–2861, Jul. 2018.

[11] P. P. Vergara, J. C. López, L. C. da Silva, and M. J. Rider, "Security-constrained optimal energy management system for three-phase residential microgrids," *Electric on Power Systems Research*, vol. 146, pp. 371–382, May 2017.

[12] L. I. Minchala-Avila, L. Garza-Castañón, Y. Zhang, and H. J. A. Ferrer, "Optimal energy management for stable operation of an islanded microgrid," *IEEE Transactions on Industrial Informatics*, vol. 12, no. 4, pp. 1361–1370, Aug 2016.

[13] F. Meng, B. Chowdhury, and M. Chamanamcha, "Three-phase optimal power flow for market-based control and optimization of distributed generations," *IEEE Transactions on Smart Grid*, vol. 9, no. 4, pp. 3691–3700, July 2018.

[14] K. H. Youssef, "Power quality constrained optimal management of unbalanced smart microgrids during scheduled multiple transitions between grid-connected and islanded modes," *IEEE Transactions on Smart Grid*, vol. 8, no. 1, pp. 457–464, Jan 2017.

[15] D. E. Olivares, C. A. Cañizares, and M. Kazerani, "A centralized energy management system for isolated microgrids," *IEEE Transactions on Smart Grid*, vol. 5, no. 4, pp. 1864–1875, Jul. 2014.

[16] R. Fourer, D. Gay, and B. Kernighan, *AMPL: A Modeling Language for Mathematical Programming*, 2nd ed. North Scituate, MA, USA: Duxbury press, 2003.

[17] R. H. Byrd, J. Nocedal, and R. A. Waltz, "Knitro: An integrated package for nonlinear optimization," in *Large-scale nonlinear optimization*. New York, NY: Springer, 2006, pp. 35–59.

[18] J. S. Giraldo, J. A. Castrillon, and C. A. Castro, "Energy management of isolated microgrids using mixed-integer second-order cone programming," in *IEEE PES General Meeting*, Chicago, IL, 16-20 July, 2017.

[19] N. Amjady, F. Keynia, and H. Zareipour, "Short-term load forecast of microgrids by a new bilevel prediction strategy," *IEEE Transactions on Smart Grid*, vol. 1, no. 3, pp. 286–294, Dec. 2010.

[20] L. Gigoni, A. Betti, E. Crisostomi, A. Franco, M. Tucci, F. Bizzarri, and D. Mucci, "Day-ahead hourly forecasting of power generation from photovoltaic plants," *IEEE Transactions on Sustainable Energy*, vol. 9, no. 2, pp. 831–842, April 2018.

[21] T.-H. Chen, M.-S. Chen, T. Inoue, P. Kotas, and E. A. Chebli, "Three-phase cogenerator and transformer models for distribution system analysis," *IEEE Transactions on Power Delivery*, vol. 6, no. 4, pp. 1671–1681, Oct. 1991.

[22] R. H. Park and B. L. Robertson, "The reactances of synchronous machines," *Transactions of the American Institute of Electrical Engineers*, vol. 47, no. 2, pp. 514–535, April 1928.

[23] J. Tamura, I. Takeda, M. Kimura, M. Ueno, and S. Yonaga, "A synchronous machine model for unbalanced analyses," *Electrical engineering in Japan*, vol. 119, no. 2, pp. 46–59, Apr. 1997.

[24] H. C. Tay and M. F. Conlon, "Development of an unbalanced switching scheme for a current source inverter," *IEE Proceedings - Generation, Transmission and Distribution*, vol. 147, no. 1, pp. 23–30, Jan 2000.

[25] V. Vekhande, V. Kanakesh, and B. G. Fernandes, "Control of three-phase bidirectional current-source converter to inject balanced three-phase currents under unbalanced grid voltage condition," *IEEE Transactions on Power Electronics*, vol. 31, no. 9, pp. 6719–6737, Sep. 2016.

[26] W. H. Kersting, "Radial distribution test feeders," *IEEE Transactions on Power Systems*, vol. 6, no. 3, pp. 975–985, Aug. 1991.